Original articles

Structural and spectroscopic studies of epitaxially overgrown GaN, n-GaN, and n+-GaN contact layers

P. V. Seredin[1✉], D. L. Goloshchapov[1], D. E. Kostomakha[1], Y. A. Peshkov[1], N. S. Buylov[1], A. A. Gaivoronskaya[1], A. M. Mizerov[2], S. N. Timoshnev[2], M. S. Sobolev[2], E. V. Ubyivovk[3], V. I. Zemlyakov[4], P. P. Kutsko[5], P. L. Parmon[5]

[1]Voronezh State University,
Universitetskaya pl. 1, Voronezh 394018, Russian Federation

[2]Alferov University,
8/3 Khlopina st., St. Petersburg 194021, Russian Federation

[3]Saint-Petersburg State University,
7-9 Universitetskaya emb., St. Petersburg 199034, Russian Federation

[4]National Research University of Electronic Technology,
1, Shokin Square, Zelenograd, Moscow 124498, Russian Federation

[5]Research Institute of Electronic Technology,
5 Staryh Bolshevikov st., Voronezh 394033, Russian Federation

Abstract

The paper demonstrates that the technology of plasma-assisted molecular beam epitaxy (PA MBE) can be used to form epitaxially overgrown GaN, n-GaN, and n+-GaN contact layers with a high structural quality on virtual GaN/c-Al_2O_3 substrates under Ga-enriched conditions at relatively low growth temperatures of ~700 °C.

It was shown that the initial stage of growth of the contact layers was accompanied by effective filtration of dislocations threading from the buffer GaN layer of the virtual substrate formed by MOCVD.

The values of residual stresses calculated using the data of Raman microspectroscopy indicate a high structural quality of GaN, n-GaN, and n+-GaN contact layers regardless of the level of silicon doping.

The contact resistance reduced to the pad width determined using the transmission line method for the structure with n+-GaN contact layer was ~0.11 Ohm·mm and for the n-GaN contact layer it was ~0.5 Ohm·mm.

Keywords: Molecular beam epitaxy, GaN, n-GaN, and n+-GaN contact layers, Virtual substrate, Raman microspectroscopy

✉ Pavel V. Seredin, e-mail: paul@phys.vsu.ru

Condensed Matter and Interphases / Конденсированные среды и межфазные границы   2024;26(3): 526–535

P. V. Seredin et al.   Structural and spectroscopic studies of epitaxially overgrown GaN, n-GaN , and n⁺-GaN...

1. Introduction

Many studies conducted in recent decades have been dedicated to group III nitrides (AIIIN) (third-generation semiconductors) and the extension of the range of their applications [1]. However, the key problem in creating viable AIIIN-based device technology solutions is the choice of a substrate for epitaxial synthesis and the method of integration with it [2–4]. In most cases, lattice-matched GaN substrates are not commercially viable despite the fact that they allow synthesizing GaN-based device heterostructures with better material characteristics and crystalline quality. An alternative solution to this problem is to form the active regions of AIIIN heterostructures by using virtual substrates (templates) of the GaN/substrate type, in which the buffer layer has already been synthesized on a commercially available substrate (Si, SiC, sapphire) by epitaxial technologies. Currently, two methods are mainly used to form GaN/substrate templates: metalorganic chemical vapor deposition (MOCVD) and molecular beam epitaxy (MBE) [3].

The second important issue in the development of AIIIN-based devices is the formation of ohmic contacts, which not only provide the connection between the device structure and the signal processing circuitry, but also are the basis for further improving the performance of final devices. The ohmic contact between metal and semiconductor must not only be compatible, but also durable and temperature stable, [5] taking into account the type of conductivity of the contact layer and technological postoperations.

The formation of high-quality ohmic contact in devices based on wide-gap AIIIN compounds is still an unresolved problem [6]. Defects in AIIIN layers and the tendency to metal oxidation at high temperatures can also affect the contact

properties. Therefore, studies aimed at reducing the contact resistance during the formation of ohmic contacts in AIIIN heterostructures are becoming increasingly relevant today.

Currently, there are a number of technological solutions to reduce the contact resistance, including the use of Ti/Al/X/Au multilayers [7]. It was also shown that the formation of fully buried Ti-based ohmic contacts results in good values of contact resistivity [6]. However, along with the traditional technology of annealing ohmic contacts [5], a wide range of studies are currently being conducted to create ohmic contacts without using the procedure of high-temperature annealing, or so-called non-annealed ohmic contacts [8–13]. In particular, papers [10–13] show that it is possible to form such contacts with a relatively low contact resistance by the epitaxial overgrowth of highly silicon-doped n⁺-GaN contact layers with an electron concentration of more than $1 \cdot 10^{19}$ cm^{-3} using the PA MBE technique.

This work presents comparative studies of the structural, morphological, and electrical properties of undoped GaN and silicon-doped n-GaN and n⁺-GaN contact layers synthesized by the PA MBE technique on GaN/c-Al$_2$O$_3$ virtual substrates grown using the method of pre-epitaxial cleaning of GaN surfaces of substrates previously developed by the authors and described in detail in [14]. The review of scientific literature has shown that there have been no studies of this kind, which emphasizes the relevance of this work.

2. Materials and methods

During the study, GaN, n-GaN, and n⁺-GaN contact layers were formed using the PA MBE technique on an industrial Veeco Gen 200 setup [14]. Synthesis was carried out on

Condensed Matter and Interphases / Конденсированные среды и межфазные границы   2024;26(3): 526–535

P. V. Seredin et al.   Structural and spectroscopic studies of epitaxially overgrown GaN, n-GaN , and n+-GaN…

virtual substrates, i.e. undoped GaN layers with a thickness of about 2.5 μm grown on sapphire substrates with (0001) orientation by metal organic chemical vapor deposition (MOCVD) [18].

After MOCVD synthesis, GaN/c-Al$_2$O$_3$ virtual substrates were extracted to the atmosphere for standard preparation procedures for PA MBE layer synthesis, which are described in detail in [14].

Immediately before the start of the PA MBE growth of the contact layers, the surfaces of the virtual substrates were cleaned following the procedure in [14]. First, the pre-epitaxial cleaning of virtual substrates was carried out in the growth chamber of the PA MBE system in a flow of activated nitrogen particles with a gradual increase in the temperature of the substrate from T_S = 400 °C to T_S = 600 °C followed by exposure of the substrate surface to a flow of activated nitrogen at a fixed value of T_S = 600 °C for 1 hour. This was followed by the final procedure of GaN surface cleaning based on the deposition of several Ga monolayers on the surface of the virtual substrate followed by thermal desorption of the deposited Ga from the surface. The study involved five periods of gallium precipitation/desorption on the GaN surface of the virtual substrate heated to T_S = 700 °C, i.e. to a temperature at which there was still no intensive decomposition of GaN, however, the flow of the thermal desorption of Ga from the liquid phase was F_{Ga}^{des} ~ 0.3 μm/h [15]. During each cycle of the stage, the precipitation of gallium atoms was completed within a 10 second exposure of GaN on the surface of the virtual substrate in a gallium flow F_{Ga} ~ 0.4 μm/h, which corresponded to the precipitation of about one Ga monolayer. The Ga flow was then shut off with a valve for 10 seconds to enable thermal desorption of the precipitated gallium from the GaN surface. Throughout the procedure of gallium adsorption/desorption, there was a "linear" pattern of reflected high energy electron diffraction (RHEED) with bright and thin reflexes characteristic of a relatively smooth GaN surface.

Immediately after the pre-epitaxial cleaning of the surfaces of the virtual substrates, undoped (sample A) and silicon-doped (samples B and C) GaN layers with thicknesses of about 250 nm were grown on the virtual substrates by PA MBE

at constant values of Ts = 700 °C, F_{Ga} ~ 0.25 μm/h, F_N ~ 0.05 μm/h and different temperatures of the silicon effusion source T_{Si} = 1,020-1,110 °C. The general scheme of samples with GaN, n-GaN, and n+-GaN contact layers is shown in Fig. 1.
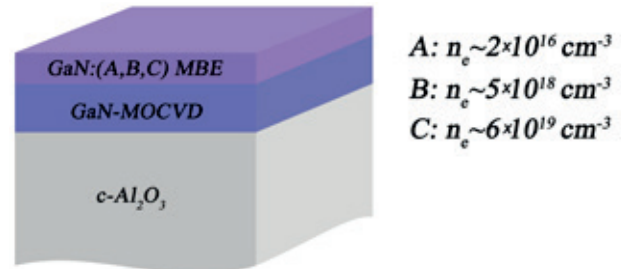
Fig. 1. Schematic representation of heterostructures with contact layers: sample A – GaN; sample B – n-GaN; sample C – n+-GaN

The GaN/c-Al$_2$O$_3$ virtual substrate with a precisely oriented c-Al$_2$O$_3$(0001) substrate were used to synthesize samples A and C, while the c-Al$_2$O$_3$ substrate with a deviation of 0.5° from [0001] direction was used to produce sample B.

The crystal structure of the samples was studied using high-resolution X-ray diffraction using a DRON-8T X-ray diffractometer with Cu$K\alpha$ radiation and an angular reproducibility of ± 0.0001°.

A RamMics 532 Raman microscope (EnSpectr, Moscow, Russia) with a radiation wavelength of 532 nm was used to obtain Raman spectra. The scanning was carried out using a 20× lens, the focal spot size of ~ 8 μm, and power of 30 mW. Raman spectra were recorded in the (xy)$^-$ geometry in the range of 100–2,000 cm^{-1} and a spectral resolution of 1 cm^{-1}. The position of the lines and the values of the full width at half maximum (FWHM) for both the GaN and Al$_2$O$_3$ layers was determined by approximating the maxima using a set of Voigt functions [16]. OriginPro software was used for processing. Spectral position of the maxima of the Raman lines was determined by measuring the position of the LO-mode of the Si calibration plate. Calibration was performed both before and after each sample measurement using a ×20 lens.

The quality of surface and hetero-interfaces was studied using scanning transmission electron microscopy (STEM) and high angular annular dark-field scanning transmission electron microscopy (*HAADF*-STEM) on a Zeiss Libra 200

Condensed Matter and Interphases / Конденсированные среды и межфазные границы   2024;26(3): 526–535

P. V. Seredin et al.   Structural and spectroscopic studies of epitaxially overgrown GaN, n-GaN , and n⁺-GaN...

FE transmission electron microscope with an accelerating voltage of 200 keV.

Ohmic contacts were metalized on a Kurt J. Lesker AXXIS unit for the electron-beam sputtering of metals.

Electrophysical measurements were performed at room temperature in a four-probe van der Pauw configuration on an Ecopia HMS-3000 measurement system.

Contact resistance was measured using the transmission line method (TLM).

3. Results and discussion

The characteristics of the epitaxial layers of GaN, such as surface structure and morphology, crystalline perfection, and density of the threading dislocations, play an important role in determining the characteristics of the heterostructure. Therefore, the surface and hetero-interface were first studied.

Images of the surface and profile of the GaN contact layers obtained at different levels of silicon doping are shown in the STEM and HAADF-STEM images (Fig. 2). For all samples, regardless of the size of the introduced impurity, there was a good smooth surface morphology with pits or V-shaped defects evenly distributed on the surface. These defects had a characteristic shape of inverted hexagonal pyramids (see the insert to Fig. 2a). These pits formed by low-index crystallographic planes can be observed during the deposition of nitride films on various substrates [17,18].

Since GaN/sapphire templates were used to form the GaN, n-GaN, and n⁺-GaN contact layers, it is obvious that the heteropairs should have a significant discrepancy in both the parameters
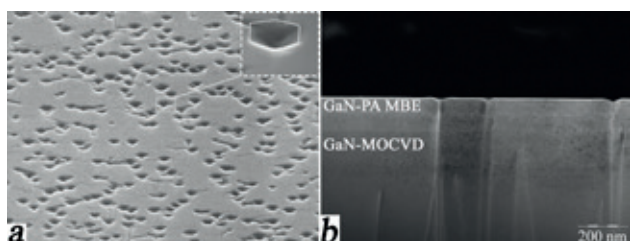
of the crystal lattices and the thermal expansion coefficients (16 and 34%, respectively). Both factors led to deformations and stress distribution gradients in the thick GaN buffer layer [19]. They were also the driving force for the formation of V-shaped pits in the upper contact epitaxial layers.

Previously, it was shown that the bottom of each pit is always associated with a threading dislocation (TD), and the density of the defects is almost always equivalent to the density of TDs [20]. Thus, the formation of V-shaped defects in the upper GaN, n-GaN, and n⁺-GaN contact layers can be explained both by the threading dislocations from the virtual substrate and the emergence of new dislocations on the interface between the surface of the virtual substrate and the GaN contact layer due to insufficiently effective pre-epitaxial cleaning of the template surface.

To study the evolution of threading dislocations during the PA MBE synthesis of GaN layers on GaN/c-Al$_2$O$_3$ templates, cross-section of one of the samples with an upper n⁺-GaN contact layer was studied by dark-field scanning transmission electron microscopy. Figure 2b shows a typical *HAADF*-STEM image of the interface between the GAN layer of the virtual substrate and the upper n⁺-GaN contact layer obtained by PA MBE.

The analysis of the *HAADF*-STEM data allows concluding that threading dislocations in the GaN, n-GaN, and n⁺-GaN contact layers were filtered. It was seen that the number of threading dislocations in the upper PA MBE layer was smaller than in the lower buffer GaN layer of the GaN/c-Al$_2$O$_3$ virtual substrate grown by MOCVD. Some of the TDs were filtered near the interface with the upper GaN contact layer, though some dislocations were still present.

The observed effect of filtration of threading dislocations may be due to the evolution of the surface morphology of the GaN contact layer at the initial stage of PA MBE synthesis on the GaN surface of the virtual substrate. In particular, the relatively low substrate temperatures used in the PA MBE synthesis of GaN could lead to the formation of three-dimensional GaN nucleation islands, which quickly grew and coalesced into a continuous GaN layer with a smooth surface

Fig. 2. Image of sample C, in which the contact n+-GaN layer was synthesized by the МПЭ ПА method on a virtual GaN/c-Al$_2$O$_3$ substrate under Ga-enriched growth conditions: STEM image of the surface (a); HAADF-STEM image of the heterointerface (b)

Condensed Matter and Interphases / Конденсированные среды и межфазные границы 2024;26(3): 526–535

P. V. Seredin et al. Structural and spectroscopic studies of epitaxially overgrown GaN, n-GaN , and n⁺-GaN...

morphology, as shown in [21]. However, during the initial stage of the island PA MBE growth of GaN, it became energetically more advantageous for the TDs to deviate from the initial vertical direction of their propagation [22]. The energy gain was due to a reduction in the TD energy since the line of the threading dislocation became shorter when it deviated to the edge of the island as compared to the energy of dislocations propagating in the direction of the GaN layer growth.

In addition, TEM studies of the synthesized samples also showed that there were no additional defects in the GaN, n-GaN, and n⁺-GaN contact layers, which could appear as a result of insufficiently effective cleaning of the surface of the GaN MOCVD layer of the virtual substrate from foreign atoms or due to surface degradation that could occur during the process of pre-epitaxial cleaning. This indicates the effectiveness of the used method of pre-epitaxial cleaning of the GaN surface of the virtual substrate.

The crystalline structure and the quality of epitaxial heterostructures were studied using high-resolution X-ray diffraction (XRD), which can provide direct information on the effect of silicon impurity on the crystalline properties of the AIIIBV and AIIIN semiconductors [23, 24]. Figure 3 shows the results of XRD measurements over a wide range of Bragg angles.

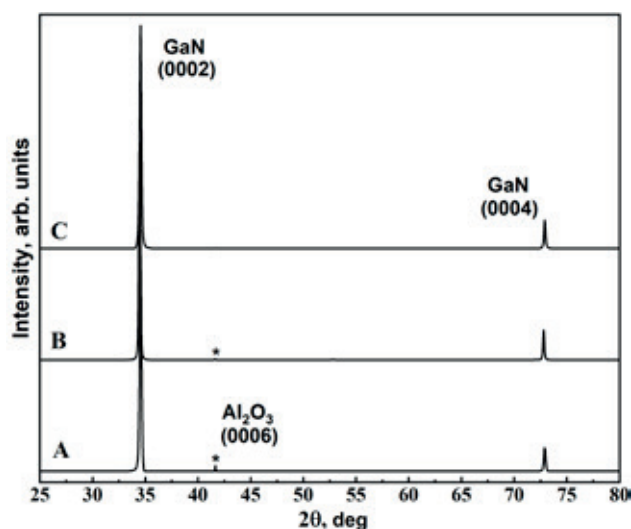**Fig. 3.** XRD 2θ-scans for samples with GaN, n-GaN and n+-GaN contact layers. Reflexes from the substrate are indicated by the index*
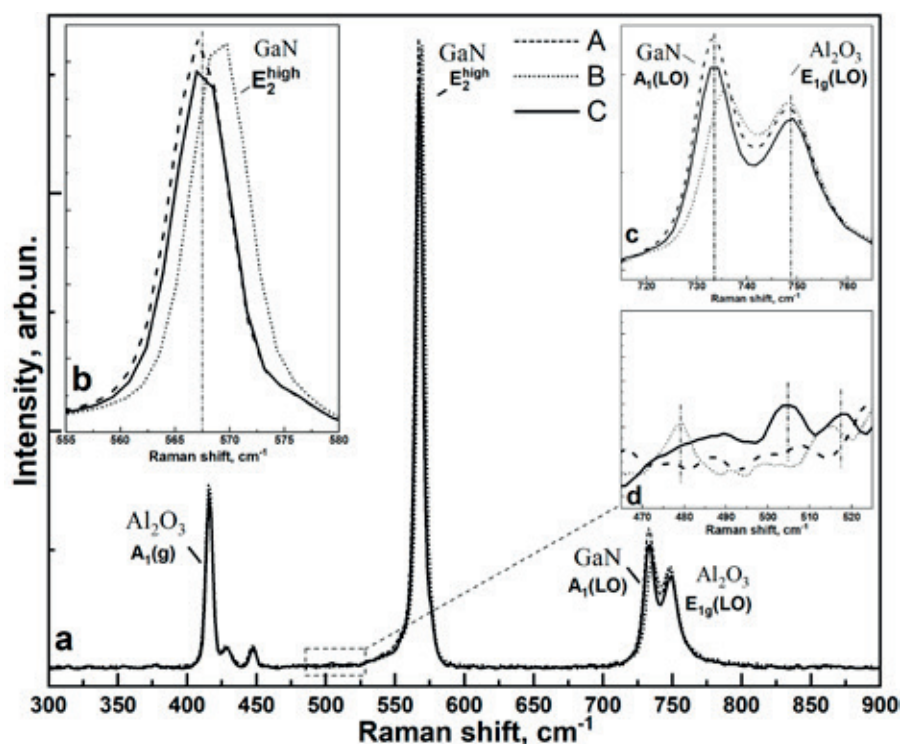
XRD 2θ-scans of all samples had maxima that also belonged to 0002 and 0004 GaN reflections with a wurtzite lattice. However, the scans also showed low-intensity reflexes belonging to the sapphire substrate. The presence of diffraction maxima of the same basal series on XRD scans suggests the monocrystalline state of the epitaxial GaN layers.

Additional structural information on the properties of the GaN, n-GaN, and n⁺-GaN contact layers was obtained by Raman spectroscopy, which allows studying the features of the crystal structure of thin epitaxial films and their perfection on the scale of crystal lattice parameters [25]. The Raman spectra of the samples are shown in Fig. 4. The Raman spectra shown in Figure 4 are typical of the *c* -plane (0001) of the GaN single crystal. They have maxima of about ~567 and 734 cm⁻¹ (Fig. 4a,b), which, in accordance with the group theory for GaN with a wurtzite crystal lattice, are transverse A_1(TO) and E_2^{high} phonon modes [26, 27]. However, the peaks present in the spectra in the region of 415 cm⁻¹ and 750 cm⁻¹ are typical characteristic longitudinal optical (LO) modes with A_{1g} and E_{1g} (LO) symmetry, which belong to the sapphire substrate [28].

Attention should be paid to another spectral feature observed in Raman scattering for the n-GaN and n⁺-GaN contact layers (samples B and C, see insert to Fig. 4d). In the region of 465–500 cm⁻¹, there was a low-intensity shoulder, the appearance of which was associated with a high level of silicon impurity in the n-GaN and n⁺-GaN contact layers. It was previously shown that the appearance of this phonon mode in the Raman spectra is associated with the formation of Si clusters in various materials [29, 30]. It should also be noted that n⁺-GaN had low-intensity Raman bands in the region of 505 and 517 cm⁻¹. According to [29, 30], the appearance of these oscillations in the Raman spectra suggests the formation of both silicon nanocrystals of various sizes and amorphous silicon.

The frequency position of active oscillations from GaN and c-Al₂O₃ in Raman spectra recorded using a x20 lens is shown in Table 1.

According to the results of our study, the value of the full width at half maximum (FWHM) of the Raman mode E_2^{high} GaN in the spectra of the GaN, n-GaN, and n⁺-GaN contact layers was ~5.0–

Condensed Matter and Interphases / Конденсированные среды и межфазные границы   2024;26(3): 526–535

P. V. Seredin et al.   Structural and spectroscopic studies of epitaxially overgrown GaN, n-GaN , and n⁺-GaN...

Fig. 4. Raman spectra for epitaxial heterostructures with contact layers of GaN, n-GaN and n+-GaN (a) – in the full range; (b) – GaN E_2^{high} and (c) – A1(LO) modes; (d) – spectral region 465–525 cm⁻¹, in which modes associated with the formation of silicon clusters of various sizes in the contact n+-GaN layer are recorded

5.2 cm¹, which indicates their high structural quality. However, this parameter was at a level characteristic of the epitaxial layers of GaN grown on a sapphire substrate [26].

The exact position of the Raman phonon mode E_2^{high} GaN compared to the undeformed GaN single crystal was used to estimate changes and to control residual stresses in the epitaxial layers due to the high sensitivity of E_2^{high} to crystal lattice deformations [31]. The following typical formula was used to estimate the value of residual biaxial stresses in the epitaxial contact layers:

$$\Delta\omega = k\sigma_{xx}. \tag{1}$$

Here, $\Delta\omega$ is the Raman shift of the mode frequency E_2^{high} GaN, σ_{xx} is the value of the residual biaxial stress in the GaN epitaxial film, k is the conversion ratio of biaxial stress to the Raman shift. The value of the conversion ratio for E_2^{high} GaN mode was 4.3 (cm⁻¹· GPa⁻¹) [32].

According to the results, the value of residual stresses in the GaN contact layer (sample A) was at the level of σ_{xx} ~ 0.1 GPa. A similar small value of σ_{xx} ~ 0.11 GPa was observed for the n⁺-GaN layer (sample C), which indicated a high degree of stress relaxation. What is more, the obtained results correlate with the known data on residual deformation in Si-doped GaN layers when grown

Table 1. The frequencies and full width at half maximum (FWHM) of the main oscillations observed in the Raman spectra of the GaN, n-GaN, and, n⁺-GaN contact layers

| Sample | Modes of Raman spectra | | | | Biaxial stress σ_{xx}, GPa |
	Al_2O_3 $A_1(g)$ ω, cm⁻¹	GaN E_2^{high} ω/FWHM, cm⁻¹	GaN $A_1(LO)$ ω/FWHM, cm⁻¹	Al_2O_3 $E_{1g}(LO)$ ω, cm⁻¹	
A (GaN)	415.6	567.0/5.1	732.6/7,9	747.5	0.11
B (n-GaN)	415.6	569.3/5.0	735.2/9,3	748	0.42
C (n⁺-GaN)	415.6	567.2/5.2	732.6/7,9	747.5	0.07

Condensed Matter and Interphases / Конденсированные среды и межфазные границы   2024;26(3): 526–535

P. V. Seredin et al.   Structural and spectroscopic studies of epitaxially overgrown GaN, n-GaN , and n$^+$-GaN…

on sapphire substrates [33]. However, the residual biaxial stresses in the n-GaN layer (sample B) were at a higher level of σ_{xx} ~ 0.4 GPa, which was probably due to the use of a misoriented sapphire substrate when creating a GaN/c-Al$_2$O$_3$ virtual substrate (see Methods).

During the last stage of the studies, ohmic Ti/Al contacts (20/100 nm) were formed on the surface of the samples using magnetron sputtering. After that, the mobility and concentration of carriers and resistivity were determined according to Hall measurements using the van der Pauw method. The results are given in Table 2.

Table 2. Hall measurement data by the van der Pauw method

Sample	Mobility of carriers cm^2/Vs	Carrier concentration, cm cm^{-3}	Resistivity Ohm·cm
A (GaN)	–	2·10^{16}	–
B (n-GaN)	265	−5·10^{18}	4.7·10^{-2}
C (n$^+$-GaN)	105	−6·10^{19}	1·10^{-2}

The contact pads of the test structure of ohmic contacts had an annular geometry with a length of the outer circumference of 400 μm. Using such topology allowed measuring contact resistance without isolating the active elements [34]. As a result, using the transmission line method (TLM) in accordance with [35] allowed determining the contact resistance reduced to the pad width, which for the structure with the n$^+$-GaN contact layer (sample C) was ~ 0.11 Ohm·mm, and for the n-GaN contact layer (sample B) ~ 0.5 Ohm·mm. Both values are in agreement with the results of the van der Pauw method (see Table 2).

It should be noted that it appeared challenging to measure the Hall characteristics for the structure with the GaN contact layer (sample A) due to the high values of resistivity (~ 1·10^4 Ohm·cm), which may indicate a sufficiently low intrinsic conductivity of this layer.

4. Conclusions

The study showed that plasma-assisted molecular beam epitaxy can be used to create overgrown GaN, n-GaN, and n$^+$-GaN contact layers on GaN/c-Al$_2$O$_3$ virtual substrates under Ga-enriched conditions. This involves effective filtration of dislocations threading from the buffer GaN layer of the virtual substrate formed by MOCVD.

Residual stresses calculated using the data of Raman microspectroscopy indicate a high structural quality of GaN, n-GaN, and n$^+$-GaN contact layers regardless of the level of silicon doping.

Contact resistance reduced to the pad width determined by the transmission line method for the structure with the n$^+$-GaN contact layer was ~ 0.11 Ohm·mm, and for the n-GaN contact layer it was ~ 0.5 Ohm·mm.

Contribution of the authors

The authors contributed equally to this article.

Conflict of interests

The authors declare that they have no known competing financial interests or personal relationships that could have influenced the work reported in this paper.

References

1. Liu A.-C., Lai Y.-Y., Chen H.-C., Chiu A.-P., Kuo H.-C. A Brief overview of the rapid progress and proposed improvements in gallium nitride epitaxy and process for third-generation semiconductors with wide bandgap. *Micromachines*. 2023;14(4): 764. https://doi.org/10.3390/mi14040764

2. Elwaradi R., Mehta J., Ngo T. H., … Cordier Y. Effects of GaN channel downscaling in AlGaN–GaN high electron mobility transistor structures grown on AlN bulk substrate. *Journal of Applied Physics*. 2023;133(14): 145705. https://doi.org/10.1063/5.0147048

3. Zeng X., Wu Y., He G., Zhu W., Ding S., Zeng Z. High-pure AlN crystalline thin films deposited on GaN at low temperature by plasma-enhanced ALD. *Vacuum*. 2023;213: 112114. https://doi.org/10.1016/j.vacuum.2023.112114

4. Yang L., Huang W., Wang D., … Wang X. AlN/GaN HEMTs with fmax exceeding 300 GHz by using Ge-doped n++GaN ohmic contacts. *ACS Applied Electronic Materials*. 2023;5(9): 4786–4791. https://doi.org/10.1021/acsaelm.3c00555

5. Wu C.-Y., Chao T.-S., Chou Y.-C. A high thermal stability ohmic contact for GaN-based devices. *Nanoscale Advances*. 2023;5(19): 5361–5366. https://doi.org/10.1039/D3NA00491K

6. Greco G., Iucolano F., Roccaforte F. Ohmic contacts to gallium nitride materials. *Applied Surface Science*. 2016;383: 324–345. https://doi.org/10.1016/j.apsusc.2016.04.016

Condensed Matter and Interphases / Конденсированные среды и межфазные границы   2024;26(3): 526–535

P. V. Seredin et al.   Structural and spectroscopic studies of epitaxially overgrown GaN, n-GaN , and n⁺-GaN...

7. Liu Y. Recent research on ohmic contacts on GaN-based materials. *IOP Conference Series: Materials Science and Engineering*. 2020;738(1): 012007. https://doi.org/10.1088/1757-899X/738/1/012007

8. Ambacher O. Growth and applications of group III-nitrides. *Journal of Physics D: Applied Physics*. 1998;31(20): 2653–2710. https://doi.org/10.1088/0022-3727/31/20/001

9. Yue Y., Hu Z., Guo J., ... Xing H. InAlN/AlN/GaN HEMTs with regrown ohmic contacts and f_T of 370 GHz. *IEEE Electron Device Letters*. 2012;33(7): 988–990. https://doi.org/10.1109/LED.2012.2196751

10. Hong S.J., Kim K. (Kevin). Low-resistance ohmic contacts for high-power GaN field-effect transistors obtained by selective area growth using plasma-assisted molecular beam epitaxy. *Applied Physics Letters*. 2006;89(4): 042101. https://doi.org/10.1063/1.2234566

11. Zheng Z., Seo H., Pang L., Kim K. (Kevin). Nonalloyed ohmic contact of AlGaN/GaN HEMTs by selective area growth of single-crystal n+-GaN using plasma assisted molecular beam epitaxy. *Physica Status Solidi (a)*. 2011;208(4): 951–954. https://doi.org/10.1002/pssa.201026557

12. Guo J., Cao Y., Lian C., ... Xing H. (Grace). Metal-face InAlN/AlN/GaN high electron mobility transistors with regrown ohmic contacts by molecular beam epitaxy. *Physica Status Solidi (a)*. 2011;208(7): 1617–1619. https://doi.org/10.1002/pssa.201001177

13. Bo Song, Mingda Zhu, Zongyang Hu, ... Xing H.G. Ultralow-leakage AlGaN/GaN high electron mobility transistors on Si with non-alloyed regrown ohmic contacts. *IEEE Electron Device Letters*. 2016;37(1): 16–19. https://doi.org/10.1109/LED.2015.2497252

14. Mizerov A. M., Timoshnev S. N., Nikitina E. V., ... Bouravleuv A. D. On the specific features of the plasma-assisted MBE synthesis of n+-GaN layers on GaN/c-Al$_2$O$_3$ templates. *Semiconductors*. 2019;53(9): 1187–1191. https://doi.org/10.1134/S1063782619090112

15. Brandt O., Yang H., Ploog K. H. Surface kinetics of zinc-blende (001) GaN. *Physical Review B*. 1996;54(7): 4432–4435. https://doi.org/10.1103/PhysRevB.54.4432

16. Wells R. J. Rapid approximation to the Voigt/Faddeeva function and its derivatives. *Journal of Quantitative Spectroscopy and Radiative Transfer*. 1999;62(1): 29–48. https://doi.org/10.1016/S0022-4073(97)00231-8

17. Zsebök O., Thordson J. V., Andersson T. G. Surface morphology of MBE-grown GaN on GaAs(001) as function of the N/Ga-ratio. *MRS Internet Journal of Nitride Semiconductor Research*. 1998;3: 1-11. https://doi.org/10.1557/S1092578300000867

18. Zsebök O., Thordson J. V., Gunnarsson J. R., Zhao Q. X., Ilver L., Andersson T. G. The effect of the first GaN monolayer on the nitridation damage of molecular beam epitaxy grown GaN on GaAs(001). *Journal of Applied Physics*. 2001;89(7): 3662–3667. https://doi.org/10.1063/1.1345516

19. Liao H., Wei T., Zong H.,... Hu X. Raman investigation on the surface carrier concentration of single GaN microrod grown by MOCVD. *Applied Surface Science*. 2019;489: 346–350. https://doi.org/10.1016/j.apsusc.2019.05.346

20. Lee Y.-J., Kuo H.-C., Lu T.-C., ... Lin S.-Y. Study of GaN-based light-emitting diodes grown on chemical wet-etching-patterned sapphire substrate with V-shaped pits roughening surfaces. *Journal of Lightwave Technology*. 2008;26(11): 1455–1463. https://doi.org/10.1109/JLT.2008.922151

21. Seredin P. V., Lenshin A. S., Mizerov A. M., Leiste H., Rinke M. Structural, optical and morphological properties of hybrid heterostructures on the basis of GaN grown on compliant substrate por-Si(111). *Applied Surface Science*. 2019;47(6): 1049–1060. https://doi.org/10.1016/j.apsusc.2019.01.239

22. Ruvimov S., Liliental-Weber Z., Washburn J., ... Weber E. R. Effect of N/Ga flux ratio in GaN buffer layer growth by MBE on (0001) sapphire on defect formation in the GaN main layer. *MRS Proceedings*. 1999;572: 295. https://doi.org/10.1557/PROC-572-295

23. Seredin P. V., Ternovaya V. E., Glotov A. V., ... Prutskij T. X-ray diffraction studies of heterostructures based on solid solutions Al$_x$Ga$_{1-x}$As$_y$P$_{1-y}$:Si. *Physics of the Solid State*. 2013;55(10): 2161–2164. https://doi.org/10.1134/S1063783413100296

24. Seredin P. V., Glotov A. V., Lenshin A. S., ... Rinke M. Structure and optical properties of heterostructures based on MOCVD (Al$_x$Ga$_{1-x}$As$_{1-y}$P$_y$)$_{1-z}$Si$_z$ alloys. *Semiconductors*. 2014;48(1): 21–29. https://doi.org/10.1134/S1063782614010217

25. Seredin P. V., Goloshchapov D. L., Lenshin A. S., Mizerov A. M., Zolotukhin D. S. Influence of por-Si sublayer on the features of heteroepitaxial growth and physical properties of In x Ga 1-x N/Si(111) heterostructures with nanocolumn morphology of thin film. *Physica E: Low-dimensional Systems and Nanostructures*. 2018;104: 101–110. https://doi.org/10.1016/j.physe.2018.07.024

26. Zeng Y., Ning J., Zhang J., ... Wang D. Raman analysis of E2 (High) and A1 (LO) phonon to the stress-free GaN grown on sputtered AlN/graphene buffer layer. *Applied Sciences*. 2020;10(24): 8814. https://doi.org/10.3390/app10248814

27. Davydov V. Yu., Kitaev Yu. E., Goncharuk I. N., ... Evarestov R. A. Phonon dispersion and Raman scattering in hexagonal GaN and AlN. *Physical Review B*. 1998;58(19): 12899–12907. https://doi.org/10.1103/PhysRevB.58.12899

28. Behera S., Khare A. Characterization of sapphire (α-Al$_2$O$_3$) thin film fabricated by pulsed laser deposition. In: *13th International Conference on Fiber*

Condensed Matter and Interphases / Конденсированные среды и межфазные границы   2024;26(3): 526–535

P. V. Seredin et al.   Structural and spectroscopic studies of epitaxially overgrown GaN, n-GaN , and n⁺-GaN...

Optics and Photonics. Kanpur: OSA; 2016; P1A.15. Available at: https://opg.optica.org/abstract.cfm?URI=Photonics-2016-P1A.15

29. Terekhov V. A., Terukov E. I., Undalov Y. K., ... Trapeznikova I. N. Effect of plasma oxygen content on the size and content of silicon nanoclusters in amorphous SiOx films obtained with plasma-enhanced chemical vapor deposition. *Symmetry*. 2023;15(9): 1800. https://doi.org/10.3390/sym15091800

30. Solonenko D., Gordan O. D., Le Lay G., Zahn D. R. T., Vogt P. Comprehensive Raman study of epitaxial silicene-related phases on Ag(111). *Beilstein Journal of Nanotechnology*. 2017;8: 1357–1365. https://doi.org/10.3762/bjnano.8.137

31. Park A. H., Seo T. H., Chandramohan S., ... Suh E.-K. Efficient stress-relaxation in InGaN/GaN light-emitting diodes using carbon nanotubes. *Nanoscale*. 2015;7(37): 15099–15105. https://doi.org/10.1039/C5NR04239A

32. Tripathy S., Chua S. J., Chen P., Miao Z. L. Micro-Raman investigation of strain in GaN and AlxGa1−xN/GaN heterostructures grown on Si(111). *Journal of Applied Physics*. 2002;92(7): 3503–3510. https://doi.org/10.1063/1.1502921

33. Talwar D. N., Lin H.-H., Chuan Feng Z. Anisotropic optical phonons in MOCVD grown Si-doped GaN/sapphire epilayers. *Materials Science and Engineering: B*. 2020;260: 114615. https://doi.org/10.1016/j.mseb.2020.114615

34. Klootwijk J. H., Timmering C. E. Merits and limitations of circular TLM structures for contact resistance determination for novel III-V HBTs In: *Proceedings of the 2004 International Conference on Microelectronic Test Structures (IEEE Cat. No.04CH37516)*. Awaji Yumebutai, Japan: IEEE; 2004; 247–252. Available at: http://ieeexplore.ieee.org/document/1309489/

35. Egorkin V. I., Zemlyakov V. E., Nezhentsev A. V., Garmash V. I., Kalyuzhnyi N. A., Mintairov S. A. Investigation of alloyed ohmic contacts in epitaxial tellurium-doped gallium arsenide layers. *Russian Microelectronics*. 2018;47(6): 388–392. https://doi.org/10.1134/S1063739718060045

Information about the authors

Pavel V. Seredin, Dr. Sci. (Phys.–Math.), Full Professor, Head of the Department, Department of Solid State Physics and Nanostructures, Voronezh State University (Voronezh, Russian Federation).

https://orcid.org/0000-0002-6724-0063
paul@phys.vsu.ru

Dmitry L. Goloshchapov, Cand. Sci. (Phys.–Math.), Assistant Professor, Department of Solid State Physics and Nanostructures, Voronezh State University (Voronezh, Russian Federation).

https://orcid.org/0000-0002-1400-2870
goloshchapov@phys.vsu.ru

Danila E. Kostomakha, graduate student, Department of Solid State Physic and Nanostructures, Voronezh State University (Voronezh, Russian Federation).

danilkostomaha@gmail.com

Yaroslav A. Peshkov, Cand. Sci. (Phys.–Math.), Research Assistant, Department of Solid State Physics and Nanostructures, Voronezh State University (Voronezh, Russian Federation).

https://orcid.org/0000-0003-0939-0466
tangar77@mail.ru

Nikita S. Buylov, Cand. Sci. (Phys.–Math.), Educator, Department of Solid State Physics and Nanostructures, Voronezh State University (Voronezh, Russian Federation).

https://orcid.org/0000-0003-1793-4400
buylov@phys.vsu.ru

Alisa A. Gaivoronskaya, student, Department of Solid State Physics and Nanostructures, Voronezh State University (Voronezh, Russian Federation).

alisa.a.gaivoronskaya@gmail.com

Andrey M. Mizerov, Cand. Sci. (Phys.–Math.), Leading Researcher, Alferov University (St. Petersburg, Russian Federation).

https://orcid.org/0000-0002-9125-6452
andreymizerov@rambler.ru

Sergey N. Timoshnev, Cand. Sci. (Phys.–Math.), Leading Researcher, Alferov University (St. Petersburg, Russian Federation).

https://orcid.org/0000-0002-9294-3342
timoshnev@mail.ru

Maksim S. Sobolev, Cand. Sci. (Phys.–Math.), Acting Head of the Laboratory of Nanoelectronics, Alferov University (St. Petersburg, Russian Federation).

ehttps://orcid.org/0000-0001-8629-2064
sobolevsms@gmail.com

Evgeniy V. Ubyivovk, Cand. Sci. (Phys.–Math.), Senior Researcher, Research Laboratory of Mechanics of Advanced Bulk Nanomaterials for Innovative Engineering Applications, Saint Petersburg State University (St. Petersburg, Russian Federation).

https://orcid.org/0000-0001-5828-4243
ubyivovk@gmail.com

Condensed Matter and Interphases / Конденсированные среды и межфазные границы   2024;26(3): 526–535

P. V. Seredin et al.   Structural and spectroscopic studies of epitaxially overgrown GaN, n-GaN , and n⁺-GaN...

Valeriy E. Zemlyakov, Cand. Sci. (Eng.), Leading Researcher, Laboratory of Nanoelectronics Element Base, National Research University of Electronic Technology (Moscow, Russian Federation).

https://orcid.org/0000-0001-5681-9603

vzml@rambler.ru

Pavel P. Kutsko, Cand. Sci. (Eng.), General Director, Research Institute of Electronic Technology (Voronezh, Russian Federation).

kutsko@niiet.ru

Pavel L. Parmon, Director of Quality, Research Institute of Electronic Technology (Voronezh, Russian Federation).

p.parmon @niiet.ru

Translated by Irina Charychanskaya